

Differential Interferometry for Precise Tracking of a Geosynchronous Satellite

T. Shiomi* and S. Nagai†

Radio Research Laboratory (RRL), Japan

and

S. Kozono,† Y. Arimoto,‡ and M. Isogai‡

Telecommunications Satellite Corporation of Japan

An experiment was carried out to track a geosynchronous satellite by a differential very-long-baseline interferometry (DVLBI) with a baseline 46 km long, observing seven quasars as reference radio sources. The geometrical delay observables were obtained with accuracies of 0.3 ns and 10~140 ns in the cases of satellite and quasars observations, respectively. The satellite orbit was fitted to the DVLBI observables with delay residuals of about 1 ns, where range and angle data obtained by a conventional radio tracking method were also used in the orbit determination. A covariance analysis shows that the DVLBI observables with an accuracy of 1 ns are effective to attain the orbit determination accuracy of about 100 m. A simulation shows that DVLBI with two baselines 1000 km long will furnish a prospective method of precise tracking of a geosynchronous satellite for an orbit determination with an accuracy of several tens of meters.

I. Introduction

THE necessity of highly accurate orbit determination is growing for satellites that are used in precise positioning, navigation, and Earth observations. In the geosynchronous orbit, such satellites are also being used for tracking other satellites or for locating positions of mobile radio stations on the Earth's surface.

The most familiar conventional radio tracking method of two-way ranging, however, has attained an accuracy of about 100 m at best in the position determination of a geosynchronous satellite. To improve the accuracy, many widely spread ranging stations with precisely known positions would be required. The system delays and the propagation media effects for every ranging station should be corrected accurately, which requires additional measuring equipment, and even so the effective corrections are not easily performed.

By adding VLBI observables, we can expect to obtain highly precise orbits, not only because the VLBI observables are complements to the range observables but because we can apply a differential VLBI (DVLBI) technique between the satellite and one of the natural radio sources of which the positions are known to calibrate the VLBI observables. The VLBI has another advantage in that it is applicable to almost any type of radio signals from the satellite, even to noise emissions. The usefulness of DVLBI was first proved in deep space navigation,¹ where DVLBI with baselines consisting of Deep Space Network (DSN) stations supplied observables equivalent to the angle measurements with an accuracy of about 50 nrad, which is five times as accurate as that obtained by the conventional Doppler measurements. An analysis of DVLBI navigation of a geosynchronous satellite was also made,² where baselines 6000 km long were assumed.

We performed a DVLBI experiment with a rather short baseline of 46 km as well as conventional ranging and angle

measurements of Japan's Experimental Communication Satellite (CS).³ The purpose of the experiment was to examine the effectiveness and limitations of DVLBI with a short baseline as a precise tracking method of a geosynchronous satellite. This paper describes the system of the experiment and the results of orbit determinations and covariance analysis made by using the DVLBI observables in addition to the range and angle data. An analysis of the information contents is also made for several models of DVLBI observations to evaluate quantitatively the effectiveness of the DVLBI observables. The covariance analysis also includes a simulation, in Japan, with two baselines about 1000 km long, which suggests the effectiveness of DVLBI for the position determination of CS with much improved accuracy.

II. Differential VLBI Method for Tracking a Geosynchronous Satellite

Principle of Differential VLBI

A VLBI measurement gives us the travel-time delay of a wavefront received at one of the stations from the time it was received at the other station. The delay estimate generally contains not only the geometrical delay but also other delays due to observation system noise, receivers and backend equipment, propagation media effects, and clock offset between the two stations.

A DVLBI can remove the common delays between two observations made under nearly the same conditions. Figure 1 shows a geometrical configuration of the DVLBI for tracking a geosynchronous satellite, where the satellite and a quasar are observed alternatively.

The delay estimate $\hat{\tau}_q$ of a quasar observation is described as

$$\hat{\tau}_q = \tau_q + n_q \quad (1)$$

where τ_q is the geometrical delay and n_q is an observation error.

The delay estimate $\hat{\tau}_s$ of a satellite observation is given by

$$\hat{\tau}_s = p_1 - p_2 + n_s \quad (2)$$

where p_1 and p_2 correspond to the geometrical propagation times between the satellite and VLBI stations 1 and 2, respectively, and n_s is an observation error.

Received Sept. 20, 1984; revision received Oct. 21, 1985. Copyright © American Institute of Aeronautics and Astronautics, Inc., 1985. All rights reserved.

*Chief, Radio Astronomy Applications Section, Kashima Space Research Center. Member AIAA.

†Member Technical Staff, Satellite Control Section, Kashima Space Research Center.

‡Member Technical Staff, Kimitsu Satellite Control Center.

The DVLBI observable $\hat{\tau}_o$ is defined by the difference between $\hat{\tau}_s$ and $\hat{\tau}_q$ as

$$\hat{\tau}_o = p_1 - p_2 - \tau_q + n_s - n_q \quad (3)$$

In an ideal DVLBI, the term $(n_s - n_q)$ contains no systematic error and the remaining random component can be reduced as sufficient signal-to-noise ratio of the observation is achieved. Assuming that τ_q is a known quantity, the geometrical delay $(p_1 - p_2)$ of the satellite is obtained from $\hat{\tau}_o$.

Geometrical Sensitivity of DVLBI Observable

The DVLBI observable is described using the station position vectors x_1, x_2 , the satellite position vector r , and the unit vector S in the line-of-sight to the quasar as

$$c(p_1 - p_2 - \tau_q) = \|r - x_1\| - \|r - x_2\| - S \cdot (x_2 - x_1) \quad (4)$$

where c is the light velocity. According to Eq. (4), the sensitivity of $\hat{\tau}_o$ with respect to small variations of r, x_1, x_2 , and S is formulated as

$$c\Delta\tau_o = (p_{1u} - p_{2u}) \cdot \Delta r + (S - p_{1u}) \cdot \Delta x_1 - (S - p_{2u}) \cdot \Delta x_2 - B \cdot \Delta S \quad (5)$$

where Δ is a small variation, p_{iu} the unit vector in the line-of-sight to the satellite at the station i , and B the baseline vector.

The first term of Eq. (5) shows the sensitivity of $\hat{\tau}_o$ to the satellite position. It is desirable to use a baseline that makes vector difference $(p_{1u} - p_{2u})$ large. The remaining terms denote the sensitivity of $\hat{\tau}_o$ to the station location errors and quasar position errors. It is usually true that smaller angular separation between the satellite and a quasar makes $\hat{\tau}_o$ more insensitive to the station location error. The quasar position error directly affects the DVLBI observables because quasars are used to calibrate them. In the station location error, we include not only the geodetic location data errors but also UT1 and polar motion errors. Consequently, in order to obtain accurate geometrical delay of the satellite τ_s , we need precise positions of the stations and quasars in an inertial coordinate system. Since VLBI is also used to measure such positions, DVLBI can be a highly self-calibrated method.

III. DVLBI Applied to Japan's Experimental Communication Satellite

VLBI System

A real-time VLBI called K-II VLBI system⁴ was used to observe CS. The K-II VLBI consists of two Earth stations, at Kashima and Hiraïso, of the Radio Research Laboratory, Ministry of Posts and Telecommunications, Japan. The baseline is about 46 km long and it is located near Tokyo (Fig. 2); the observation frequencies are in the 4-GHz band. The digitized and formatted observed data at Hiraïso station are transmitted via a microwave ground link to Kashima, where a real-time correlator cross-correlates the observed data, integrates the fringe-stopped correlated data for every 10 ms, and records the results on a computer tape. The observation can be made at up to five channels. The observation channel is sequentially alternated and the dwelling period of each channel is 100 ms. Some main features of the K-II system are summarized in Table 1. Our observations were made by using two channels of 4041 MHz (CH 2) and 4061 MHz (CH 3), which are within the 200-MHz bandwidth of one of the two C-band transponders of CS.

DVLBI Observations

The noise emission from the C-band transponder of CS was observed by DVLBI method for 17 hrs on June 16, 1982. Seven quasars were selected as reference natural radio sources. Figure 3 shows the viewing angles of the quasars and CS at

each observation epoch time at Kashima station. Since the baseline vector is almost in the north-south direction, the VLBI observables are sensitive to the north-south component of the satellite position and motion. In fact, the north-south component of the sensitivity vector $(p_{1u} - p_{2u})$ in Eq. (5), which is the major component, is 9.14×10^{-4} . This means that a position change 100 m of CS corresponds to a DVLBI delay change of 0.3 ns. Using the quasars, eight sets of DVLBI observations were made. A set of DVLBI observations consisted of three 10-min observations, first of a quasar, then of CS, and again of the quasar.

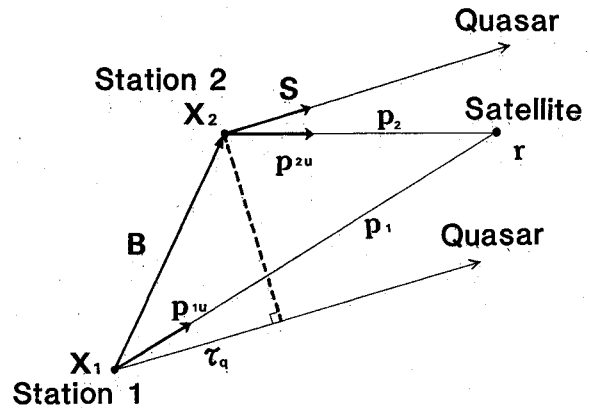


Fig. 1 Geometry of DVLBI observations.

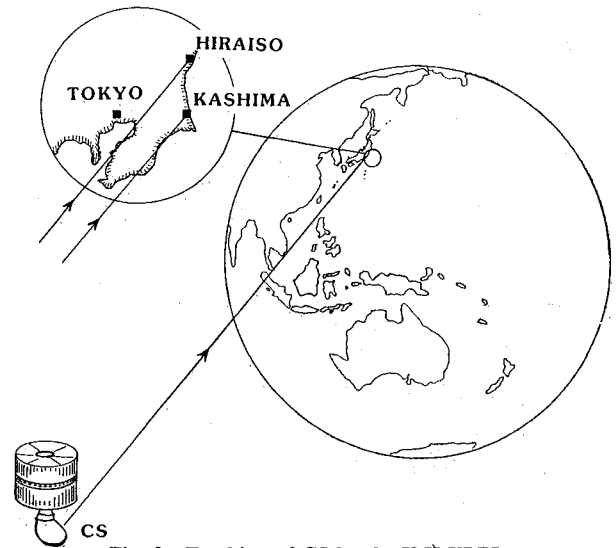


Fig. 2 Tracking of CS by the K-II VLBI.

Table 1 K-II VLBI system

VLBI stations	Kashima	Hiraïso
Receiving antenna, m	26	10
Antenna gain, dB	58.9	48.9
System noise, K	111	130
Observation frequencies, MHz	CH 1: 4031, CH 2: 4041, CH 3: 4061, CH 4: 4091, CH 5: 4131	
Bandwidth	2 MHz/CH	
Sampling rate	4 Mbits/s	
Frequency standard (stability 10 s)	Cesium (2.5×10^{-12})	Rubidium ($< 1.6 \times 10^{-12}$)
Data transmission	Raw data of Hiraïso transmitted to Kashima via microwave data link	
Correlator	Real-time correlator, lag 32 bits, integration 10 ms	

As the DVLBI observables were not sufficient by themselves for the orbit determination, we also made conventional radio trackings, that is, ranging and angle measurements. The ranging was carried out by using a 100-kHz range tone in the 4-GHz frequency band. The satellite angles were measured by a 13-m antenna that tracked the beacon signal of 19.45 GHz from CS. In order to reduce the calibration errors of atmospheric refraction and of deformations of the antenna dish and the sustaining structure, including the building on which the antenna was installed, angle data measured during the night were used as the tracking data. Figure 4 shows the observation points of those tracking data.

Accuracy of DVLBI Observations

The major random error σ_r in VLBI delay observable is evaluated by the signal-to-noise ratio (SNR)⁵ as

$$\sigma_r = 1/(\omega_{\text{eff}} \text{SNR}) \quad (6)$$

where ω_{eff} is an effective bandwidth in the delay estimation and is given as

$$\omega_{\text{eff}} = \sqrt{\sum_{i=1}^K (\omega_i - \bar{\omega})^2}, \quad \bar{\omega} = \sum_{i=1}^K \omega_i / K \quad (7)$$

where K is the number of observation channels and ω_i is the observation frequency of the channel i . SNR is given as

$$\text{SNR} = \rho \sqrt{2BT} \quad (8)$$

$$\rho = L \cdot \sqrt{\frac{T_{a1} T_{a2}}{T_{a1} T_{s2} + T_{a2} T_{s1} + T_{s1} T_{s2}}} \quad (9)$$

where T_{ai} and T_{si} are signal and noise temperatures, respectively, at the station i ; ρ is a normalized correlation amplitude;

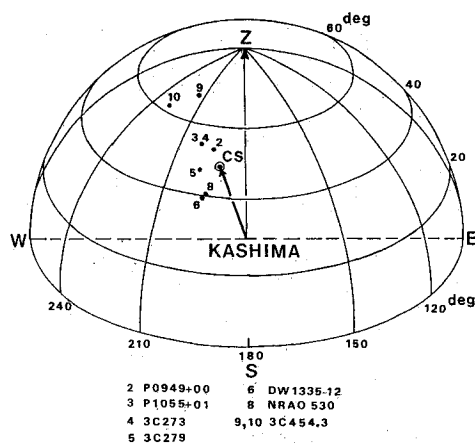


Fig. 3 Viewing angles of CS and quasars at Kashima station; 2~10 denote the quasars.

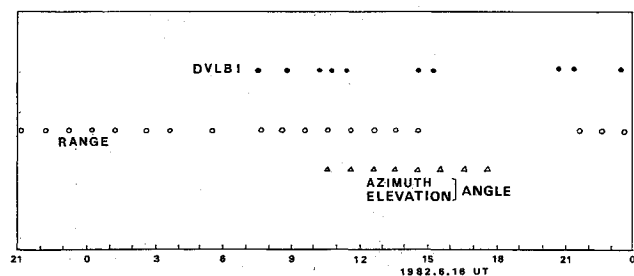


Fig. 4 Tracking data of CS.

L a coherence loss factor ($0 \leq L \leq 1$); B the observation bandwidth; and T the integration time. In the case of a CS observation σ_r is evaluated as about 0.3 ns using $\omega_{\text{eff}}/2 = 0.5$ MHz and $\text{SNR} = 1050$. The SNR value is calculated using $L = 0.4$, $T = 10$ s, $B = 2$ MHz, the system noise temperatures given in Table 1, and the signal temperatures calculated by the satellite power flux density of $1260 J_y$ ($1 J_y = 10^{-26}$ Watt/m²Hz). On the other hand, σ_r in a quasar observation is generally much larger than that in a CS observation because a quasar signal is much weaker. For example, SNR is about 7.2 for a quasar observation, where flux density $5 J_y$ and integration time $T = 30$ s are assumed, which gives $\sigma_r = 44$ ns.

Data Reduction of DVLBI Observations

The observed VLBI data of each channel were processed independently. The delay observable was estimated by simultaneous search of delay deviation $\Delta\tau$ and delay-rate deviation $\Delta\dot{\tau}$ from their predictions so that they maximize the following normalized correlation amplitude ρ_{obs} .

$$\rho_{\text{obs}} = \frac{1}{T\omega_B} \left\| \int_T \int_{\omega_B} S_{xy}(\omega, t) \exp\{-i(\omega\Delta\tau + \omega_o\Delta\dot{\tau}t)\} d\omega dt \right\| \quad (10)$$

where $S_{xy}(\omega, t)$ is a cross spectrum derived every 1 s using the predicted delay and delay rate, $\omega/2\pi$ a video frequency, t an observation epoch time, $\omega_B/2\pi$ the observation bandwidth, T the integration time, $\omega_o/2\pi$ the observation frequency in the 4 GHz band, and $\| \cdot \|$ the magnitude.

Figure 5 shows the estimated delays for all the observations of the satellite and the quasars. The integration time T was 15

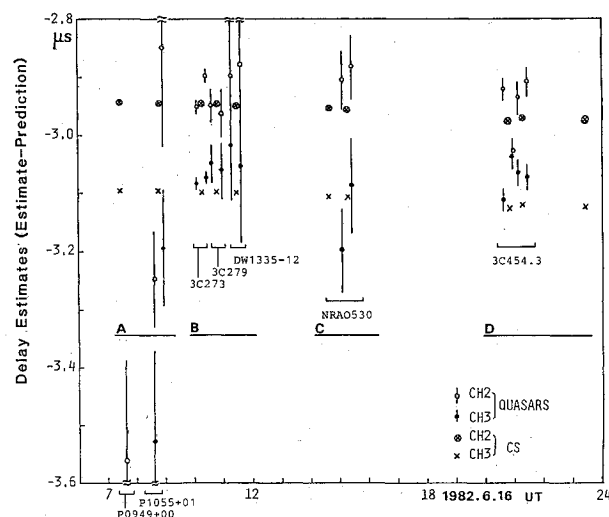


Fig. 5 Estimated delays. Vertical lines show standard deviations evaluated by correlation amplitudes; A~C denote four observation periods.

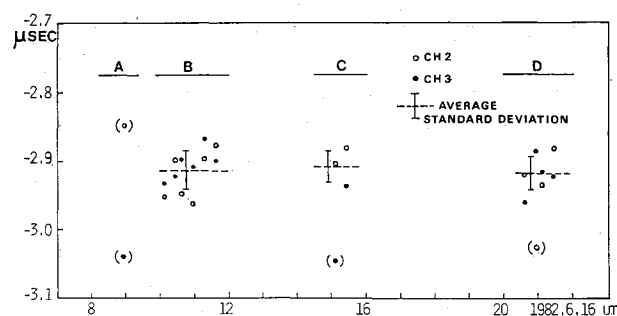


Fig. 6 System delay estimates with channel 2; (*): rejected data.

s for a CS observation and 30 s for a quasar observation. The obtained delay accuracies for the satellite and quasars agreed with the result of the theoretical evaluation given above.

Figure 5 indicates that a systematic delay difference existed between the estimated delays for the observations in channels 2 and 3. The differences were estimated using the delays of the CS observations for four observation periods A, B, C, and D defined in Fig. 5. They were 152.46, 151.32, 151.56, and 149.68 ns, respectively. Assuming that these delay differences for CS observations can also be applied to those of quasars, we converted quasar delay estimates in channel 3 into those that are equivalent to delays in channel 2. The result is shown in Fig. 6. The above assumption was applied because the observed signal of each source (CS or a quasar) had nearly the same flat power spectrum, which caused the same system delay, though the power flux itself was different from each other.

Under the assumption that the quasar delay predictions are error-free, Fig. 6 gives the system delay for channel 2. We averaged the data in the observation periods B, C, and D, and obtained the system delays, -2913.51 , -2907.96 , and -2918.18 ns, respectively. The DVLBI delay observable for CS were obtained by subtracting these system delays from the raw CS delays shown in Fig. 5.

The fairly large standard deviation of the system delay estimates were due to the insufficient accuracy of the delay estimates in the quasar observations.

IV. Orbit Determination

Results of the Orbit Determination

The DVLBI observables were added to the range and the angle data to determine the CS orbit. In the orbit determination, the observation bias of the DVLBI observables and the solar radiation reflection coefficient of the satellite (the satellite cross section multiplied by this coefficient is effective on the solar radiation pressure) were also estimated simultaneously. The bias of the DVLBI observables was introduced because of the insufficient quality of the DVLBI data. The range and angle measurements had been calibrated using an optical observation method.⁶ We used system parameters that have since been updated through orbit determinations operationally performed in the CS project.

Table 2 summarizes the results of orbit determination with four accuracy models of DVLBI observables, cases 1-4. The same weights for the range and angles observables were used in all cases, which agree with their actual characteristics. Cases 2 and 3 show that the estimated satellite position approaches that of case 1 as the assumed DVLBI delay accuracy becomes worse, while the estimates of the delay bias and the solar radiation reflection coefficient change only slightly. In other

words, the DVLBI observables become almost meaningless if their accuracy is lower than about 3 ns. Figure 7 shows the observation residuals of the range and the DVLBI delay data for case 4, where the standard deviation of DVLBI delay residuals is about 1 ns (0.3 m). Therefore it appears that the DVLBI observables obtained in our experiment might be effective in improving the orbit determination accuracy. However, the expected accuracy of the DVLBI observables was about 25 ns, as is shown in Fig. 6. So it is reasonable to consider that the small residuals in Fig. 7 are obtained because of the small amount of DVLBI observables and that our DVLBI data are not useful for a precise orbit determination. Significant causes of the insufficiency of the DVLBI data are: 1) poor accuracy of the delay data due to small SNR in the quasar observations and 2) poor sensitivity of the DVLBI delay observable to the satellite orbit due to shortness of the baseline. In the next section, covariance analyses show effects of some improvement in these two points.

Covariance Analysis

Table 3 summarizes the results of the covariance analysis using six models. The DVLBI data were not used in case a, DVLBI data with different models of accuracy were used in cases b, c, d, and a model with smaller uncertainties in station locations was used in case e. Simulated DVLBI data obtained by two baselines shown in Fig. 8 (Kashima, Wakkanai, and Yamagawa, all in Japan) were used in case f.

Case d means that if we truly obtain the DVLBI data with an accuracy of 1 ns, we can expect nearly 100-m accuracy of the orbit determination, except for the effect of the uncertainties in model parameters. In that case, we can expect 300-m accuracy, considering the effect of uncertainties in the model parameters, including 50-cm uncertainties in the station locations, which is shown in case e. In case d, the satellite position accuracy that considers the effect of the parameter uncertain-

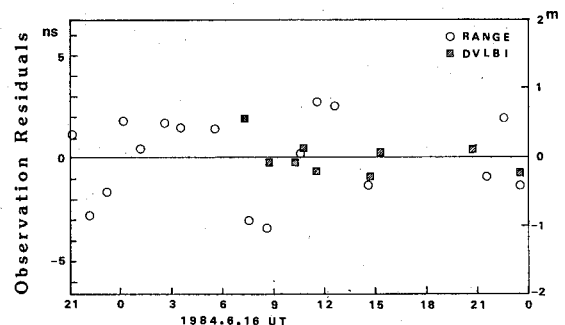


Fig. 7 Observation residuals in an orbit determination of CS.

Table 2 Result of orbit determination

	Orbit determination by case			
	1	2	3	4
Observation weight				
Range, 0.52 m				
Azimuth angle, 0.98×10^{-3} deg				
Elevation angle, 0.85×10^{-2} deg				
DVLBI delay, ns	(not used)	16.7	3.33	1.0
(m)		(5.0)	(1.0)	(0.3)
Estimated parameters				
DVLBI delay bias, ns	—	-83.79	-83.82	-83.66
Solar radiation reflection coefficient	1.5084	1.5083	1.5071	1.5060
Satellite position at epoch time		Deviation from Case 1		
X, km	41918.261	-0.002	-0.030	-0.055
Y, km	-4528.804	0.013	0.188	0.409
Z, km	-194.97	-0.037	-0.496	-0.992

ties is not improved from cases a, b, and c, although the better accuracy of the DVLBI data is assumed. This is because the uncertainties in the VLBI station locations are more telling in case d than in the other cases. Case f shows a possibility of precise orbit determination with an accuracy of nearly 70 m by a combination of the conventional radio tracking and DVLBI with two baselines nearly 1000 km long.

The information content I_c , which is defined by⁷

$$I_c = 1/2 \cdot \log_2(|P_0|/|P|) \quad (11)$$

is also shown in Table 3, where P is the six-dimensional covariance matrix of the estimated position and velocity of CS, and $| \cdot |$ denotes the determinant of a matrix. P_0 stands for the covariance with no DVLBI observables in the orbit determination. I_c is a measure of the information content of the DVLBI observables because it represents the reduction of an error ellipsoid by the information given by them. It is quantitatively clear that the more information is given by DVLBI, the more accurate are its observables. Case f shows that DVLBI delay observables with longer baselines contain much larger amounts of information even if the delay accuracy is about 3.3 ns than the amounts with a short baseline with a higher delay accuracy.

In order to improve the orbit determination accuracy within 100 m in the satellite position, it is effective to use longer baselines. It is also expected that if we use longer baselines—for example, intercontinental baselines—we can obtain an accuracy of less than 10 m in the position of the satellite.⁸ The DVLBI observables obtained using more than two baselines can determine the angular position of the satellite. It means that such DVLBI observations for about 24 h can effectively determine the orbit of a geosynchronous satellite. In our experiment, we used the range and the angle data obtained by the conventional radio tracking method as well as DVLBI data. In such a case, many types of tracking methods involved increase the number of parameters, such as

calibration factors and observation system parameters, in which uncertainties easily degrade the orbit determination accuracy. On the other hand, the DVLBI observables have an advantage in that they are essentially free from bias errors or can be calibrated by themselves. The station locations are also obtained by appropriate VLBI observations of quasars. So it would be advisable to use only DVLBI observables with truly long baselines to determine the orbit of a geosynchronous satellite with a high degree of accuracy.

In our experiment, the poor quality of the DVLBI delay observables is mainly due to the insufficient accuracy of delay estimates in the observations of quasars. Much better-quality quasar delays would require some improvement that acts to increase SNR in the VLBI system. For example, a hydrogen maser frequency standard would be effective in achieving much longer integration time. It would also be important to use a phase calibration system that makes possible a bandwidth synthesis with observations in different-frequency channels.

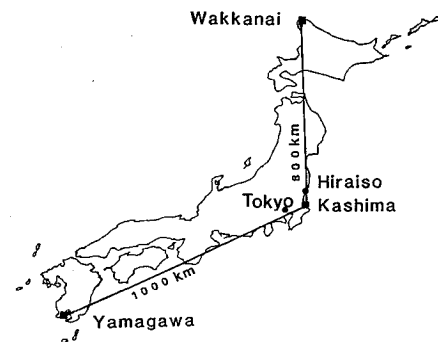


Fig. 8 An example of three long baselines assumed in Japan.

Table 3 Result of covariance analysis

	Covariance analysis by case					
	a	b	c	d	e	f ^a
Observation weight						
Range, 0.52 m						
Azimuth angle, 0.98×10^{-3} deg						
Elevation angle, 0.85×10^{-2} deg						
DVLBI delay, nsec (m)	0	16.7 (5.0)	3.33 (1.0)	1.0 (0.3)	1.0 (0.3)	3.33 (1.0)
Parameter uncertainty						
Solar radiation reflection coefficient, 0.003						
Earth's gravity constant, $0.04 \text{ km}^3/\text{s}^2$						
Station location, m	1.0	1.0	1.0	1.0	0.5	1.0
Satellite position accuracy						
Parameter uncertainties are not considered						
σ_x , m	47	46	33	18	18	2.9
σ_y , m	158	158	146	128	128	17
σ_z , m	455	446	318	129	129	20
Parameter uncertainties are considered						
σ_{xc} , m	47	46	54	96	51	8.8
σ_{yc} , m	173	172	170	367	220	65
σ_{zc} , m	469	459	463	510	278	28
Information content of DVLBI observables	0	0.13	2.09	6.74	6.74	23.6

^aDVLBI delay observables are replaced by those obtained by two baselines shown in Fig. 8.

V. Conclusion

The geosynchronous satellite CS was tracked using a differential VLBI method. Since the baseline was short and the data quality of quasar observations insufficient, the obtained DVLBI delay observables were not actually useful in improving the accuracy of orbit determinations. However, orbit determinations and covariance analysis using various error models showed the possible effectiveness of DVLBI with a delay accuracy of about 1 ns and with appropriate baselines obtained in Japan's territory for accurate orbit determinations of geosynchronous satellites. The DVLBI has these advantages: the observables are essentially free from bias errors or they can be calibrated by themselves, and the method is passive, with no necessity for uplink facilities; it is also applicable to many types of signals radiated from a satellite. Since a covariance analysis shows that a DVLBI with long and independent baselines is very effective for an accurate orbit determination, further experiments with long baselines including inter-continental ones can validate fully the usefulness of the method.

Acknowledgments

The experiment was carried out with the support of the Radio Astronomy Applications Section, Kashima Space Research Center, RRL, and of the Solar Radio Research Section, Hiraiso Branch, RRL. The authors acknowledge valuable support and advice given in every phase of the experi-

ment by Dr. N. Kawano, Mr. F. Takahashi, and Mr. K. Koike, of the Radio Astronomy Applications Section.

References

- ¹Jordan, J.F., "Deep Space Navigation Systems and Operations," ESA International Symposium on Spacecraft Flight Dynamics, May 1981.
- ²Yunck, T.P. and Wu, S.C., "Tracking Geosynchronous Satellites by Very-Long-Baseline Interferometry" *Journal of Guidance, Control, and Dynamics*, Vol. 6, Sept.-Oct. 1983, pp. 382-386.
- ³Tsukamoto, K., Otsu, Y., Kosaka, K., Shiomi, T., and Sasaoka, H., "Experimental Program and Performance of Japan's Communication Satellite (CS) and Its First Results," *IEEE Transactions on Communications*, Vol. COM-27, No. 10, 1979, pp. 1392-1405.
- ⁴Kawano, N., Takahashi, F., Yoshino, T., Koike, K., Kumagai H., and Kawajiri, N., "Development of Real-Time VLBI and Measurements of Scintillation," *Journal of Radio Research Laboratories*, Vol. 29, No. 127, July 1982, pp. 53-102.
- ⁵Whitney, A.R., "Precisions Geodesy and Astrometry Via Very-Long-Baseline Interferometry," Doctoral Thesis, Massachusetts Institute of Technology, Cambridge, Jan. 1974.
- ⁶Kawase, S., Kawaguchi, N., Tanaka, T., and Tomita, K., "Optical Calibration of geostationary Satellite Tracking Systems," *IEEE Transactions on Aerospace Electronic Systems*, AES-17, March 1981, pp. 167-172.
- ⁷Bucy, R.S. and Joseph, P.D., "Filtering for Stochastic Processes With Applications to Guidance," Interscience Publishers, John Wiley & Sons, New York, 1968.
- ⁸Border, J.S. and Donivan, F.F. Jr., "Geosynchronous Orbiter Tracking by VLBI: Demonstration Design," *Proceedings of AIAA/AAS Astrodynamics Conference*, 1984.

From the AIAA Progress in Astronautics and Aeronautics Series

SPACECRAFT RADIATIVE TRANSFER AND TEMPERATURE CONTROL—v. 83

Edited by T.E. Horton, The University of Mississippi

Thermophysics denotes a blend of the classical engineering sciences of heat transfer, fluid mechanics, materials, and electromagnetic theory with the microphysical sciences of solid state, physical optics, and atomic and molecular dynamics. This volume is devoted to the science and technology of spacecraft thermal control, and as such it is dominated by the topic of radiative transfer. The thermal performance of a system in space depends upon the radiative interaction between external surfaces and the external environment (space, exhaust plumes, the sun) and upon the management of energy exchange between components within the spacecraft environment. An interesting future complexity in such an exchange is represented by the recent development of the Space Shuttle and its planned use in constructing large structures (extended platforms) in space. Unlike today's enclosed-type spacecraft, these large structures will consist of open-type lattice networks involving large numbers of thermally interacting elements. These new systems will present the thermophysicist with new problems in terms of materials, their thermophysical properties, their radiative surface characteristics, questions of gradual radiative surface changes, etc. However, the greatest challenge may well lie in the area of information processing. The design and optimization of such complex systems will call not only for basic knowledge in thermophysics, but also for the effective and innovative use of computers. The papers in this volume are devoted to the topics that underlie such present and future systems.

Published in 1982, 529 pp., 6×9, illus., \$35.00 Mem., \$55.00 List

TO ORDER WRITE: Publications Dept., AIAA, 1633 Broadway, New York, N.Y. 10019